

# New Limits on the Ultra-high Energy Cosmic Neutrino Flux from the ANITA Experiment and Current Developments

Andrew Romero-Wolf\*, for the ANITA Collaboration

\*Department of Physics and Astronomy, University of Hawaii at Manoa, HI 96822, USA

**Abstract.** Initial results of the first flight of the Antarctic Impulsive Transient Antenna (ANITA-1) 2006-2007 Long Duration Balloon flight will be presented. The experiment searched for evidence of a diffuse flux of cosmic neutrinos above energies of  $E \approx 3 \times 10^{18}$  eV. ANITA flew for 35 days (with 15 days of good radio quiet data) looking for radio impulses due to the Askaryan effect in neutrino-induced electromagnetic showers within the Antarctic ice sheets. The early analysis reported here was performed as a blind search of the data. No neutrino candidates are seen, with no detected physics background. Model-independent upper limits based on this result begin to eliminate the highest cosmogenic neutrino models. In a background horizontal-polarization channel, this analysis detected six events consistent with radio impulses from ultra-high energy extensive air showers. Some current developments towards improving the analysis sensitivity as well as an overview of ANITA's successful second flight in 2008-2009 will also be presented.

**Keywords:** Neutrino Detection, Askaryan Effect, Radio Frequency, GZK Effect

## I. INTRODUCTION

The goal of the ANITA experiment is to provide the first detection of ultra high energy (UHE) neutrinos and, if successful, open the road towards the exciting new realm of UHE neutrino astronomy. Although an UHE ( $> 10^{18}$  eV) neutrino has not been observed, their production is predicted as a consequence of the GZK ([1],[2]) cutoff mechanism. As ultra-high energy cosmic rays (UHECR) with  $E_{CR} > 4 \times 10^{19}$  propagate they interact with the cosmic microwave background radiation via the  $\Delta$  resonance leading to the production of neutrinos, photons, and lower energy hadrons. The prediction of UHE neutrinos was first made by Berezhinsky and Zatsepin (BZ) [3]. The observation of the GZK cutoff [4] and precision measurements of the  $\Delta$  resonance interaction [5] result in a "guaranteed" UHE neutrino flux at energies  $E_\nu = 10^{17-20}$  eV in most BZ neutrino models. Given that UHE neutrinos propagate through the universe practically unattenuated, detection of this UHE neutrino flux is one of the clearest ways to reveal the nature and cosmic distribution of the UHECR sources [6], which is one of the longest-standing problems in high energy astrophysics.

A proof of concept experiment for the detection of UHE neutrinos was performed in SLAC in 2006 [7].

UHE neutrinos interacting in a dense dielectric medium produce particle showers which emit strong coherent Cherenkov pulses at radio frequencies [8]. The radio emission can be detected from far away if the medium is radio transparent, as is the case for ice. Coherent radio Cherenkov pulses were produced by  $10^{19}$  eV electron bunches in a block of ice and detected with the ANITA instrument in SLAC's end station A.

ANITA had a successful 35 day flight over Antarctica in 2007 (ANITA-1) and an improved second 30 day flight in 2009 (ANITA-2). In the following, neutrino flux limits from the first completed analysis of the ANITA-1 data are presented. Current developments towards a refined lower threshold analysis for ANITA-1 are discussed. Finally, the ANITA-2 instrument and flight performance is shown.

## II. FIRST ANITA FLIGHT AND RESULTS

The details of the ANITA-1 instrument and flight system, far too lengthy and complex to cover in the present work, are contained in [9]. The interested reader can find more information on the instrument performance during the flight, estimates of the overall sensitivity of the instrument to neutrino fluxes, and discussions of possible backgrounds.

The ANITA-1 payload was launched from the Long Duration Balloon facility at Williams Field, Antarctica near McMurdo station, on December 15, 2006, and flew for 35 days. The ANITA-1 flight had an unusual trajectory resulting in a large fraction of time being spent over West Antarctica where the exposure to ice volume is smaller than the rest of the continent. In addition, the two largest occupied stations in Antarctica, McMurdo and Amundsen-Scott, were often in the field of view subjecting the payload to higher levels of anthropogenic electromagnetic interference than expected. Despite these complications, the payload acquired a livetime of 17.3 days with a mean ice depth in the field of view of 1.2 km. ANITA-1 was thus exposed to an ice volume of  $\sim 1.6$  M km<sup>3</sup>. The ANITA-1 instrument is composed of 32 dual-polarized horn antennas with 10 dBi directive gain and 45° beam width. The payload is arranged in two groups of 16 cylindrically symmetric antenna arrays for full azimuthal coverage. All antennas have a cant angle of 10° with one group located  $\sim 3$  meters directly above the other to optimize the instrument's sensitivity to radiation pointing near the Antarctic horizon. The ANITA instrument has a frequency range of 200 - 1200 MHz. Each horn antenna and polarization

TABLE I  
EVENT TOTALS VS. ANALYSIS CUTS AND ESTIMATED SIGNAL  
EFFICIENCIES FOR UNBLINDED ANITA-1 DATA SET.

Cut requirement	passed:	total	Hpol	Vpol	Efficiency
(0) Hardware-Triggered		~8.2M	...	...	...
(1) Upcoming plane wave		32308	15997	16311	0.93
(2) Impulsive broadband		19695	10095	9600	0.98
(3) Isolated from other events		9	8	1	0.94
(4) Isolated from camps		6	6	0	0.96
(5) Vpol dominant		0	0	0	0.99

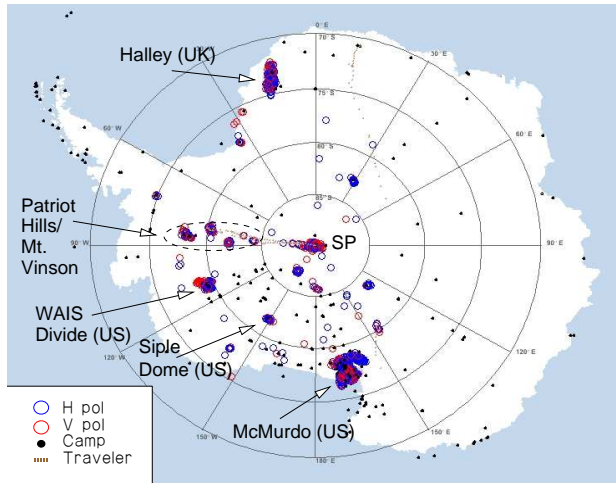


Fig. 1. Plot of all reconstructed events, in both horizontal and vertical polarization; major Antarctic stations are indicated on the map.

channel (64 total) has a series of band pass filters, a 75 dB amplifier, and is split between a trigger path and a digitization path which takes 260 samples at a rate of  $2.6 \times 10^9$  samples per second.

The trigger decision works on three levels that, together, require that the incident radiation to be broadband and geometrically consistent with plane wave incidence. The trigger thresholds are adjusted during flight for a trigger rate of 5 Hz on thermal noise. These events are incoherent in phase and produce a negligible background to actual coherent radio impulses. The signal efficiency of the trigger is 50% at a peak signal to rms noise ratio (SNR) of 5.5 and 100% at an SNR of 7. The details of the ANITA-1 trigger are discussed in [9]. The data analysis and event reconstruction rely on the precise timing resolution (45-60 ps) of the instrument. The incident direction of the signal is reconstructed from the timing between antennas and their geometry. In the first analysis presented here, the timing between antennas is estimated from the peak of the cross-correlation between the waveforms of six adjacent antennas with detectable signals. The angular precision of the reconstructed direction is  $0.2^\circ \times 0.8^\circ$  in elevation and azimuth [9]. The direction and its associated uncertainty is then mapped onto the Antarctic ice surface by reference to onboard payload navigation instruments.

An analysis blinding procedure was implemented where the analysis cuts were optimized on a 10% randomized sample of the entire data set. Once the

cuts were fixed, the remaining 90% was opened to the analysts. The cuts proceed as follows: **(1)** Events that do not reconstruct to a plane wave pointing below the horizon are rejected. **(2)** Events that have non-impulsive waveforms are rejected. **(3)** Events that have continental projections that cluster with one another within reconstruction errors or 50 km radius, whichever is greater, are rejected. True source candidates must be single, isolated events. **(4)** Events that point to any known active or inactive station, camp, aircraft flight path, or expedition traverse path, to within reconstruction angular errors, or 50 km radius, whichever is greater, are rejected. Inactive and abandoned camps are included since left-over equipment might serve as a site for electromagnetic discharges which could be mistaken for signals. **(5)** Events whose radio waveforms are not predominantly vertically polarized (Vpol) are rejected since they are inconsistent with events generated by Askaryan process and Fresnel transmission through the ice surface. By similar considerations, strongly horizontally polarized (Hpol) are likely to originate from above the ice.

Table I shows the results of the total event sample and signal efficiency for each cut. The 10% initial sample is included in the totals. Note that the isolation cut (3) is the single most stringent criterion in rejecting impulsive events, and this shows that the vast majority of triggers are not single, isolated events. Signal efficiency for each cut was tested with a data set of simulated events. The final energy-averaged efficiency of all cuts is estimated to be 81%.

In figure 1 we show a map of reconstructed ANITA-1 events superposed on the Antarctic continent. The figure shows the vast majority of events are correlated to a small number of stations. All but 6 Hpol events were removed by the isolation (3) and base (4) cuts. The possibility of the 6 Hpol events originating from extended air showers is discussed in [10]. The analysis cuts have left no neutrino candidates.

Figure 2 shows the resulting model-independent 90% CL limit on neutrino fluxes with Standard Model cross-sections [11]. The approach used to obtain this result is described in Refs. [12], [13]. The net livetime and 81% analysis efficiency are included. Exclusion of the volume of ice near all camps and events reduces the net effective volume by a few percent. Experimental systematics that affect the expected signal features lead to uncertainties of order a factor of two on the limit. These model-independent limits are calibrated such that a model spectrum that matched the limit over one decade of energy would yield approximately 2.3 events; this choice is appropriate to smoothly varying models. ANITA-1 had roughly equal sensitivity to  $\nu_e$ ,  $\nu_\mu$ ,  $\nu_\tau$  and the flavors should be equally mixed to first order via oscillations. The limits are thus averaged over all three neutrino flavors. Given the large number of BZ neutrino models, only an approximate set of predicted bands are plotted. Table II gives the total number of events expected from a representative sample of BZ

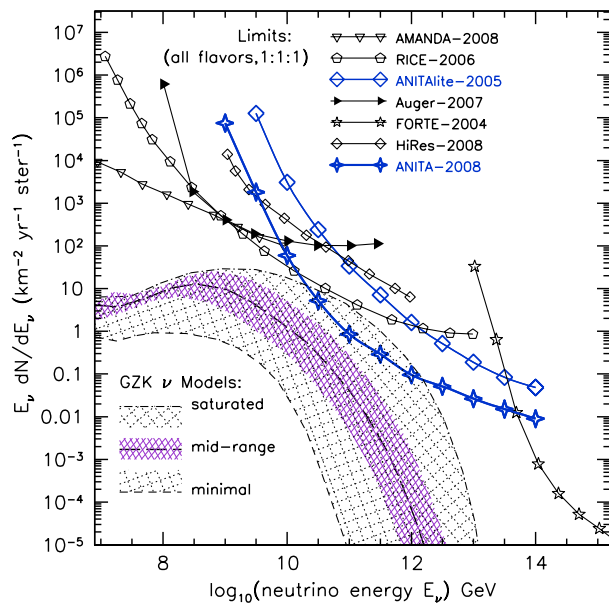


Fig. 2. ANITA-1 limits based on no surviving candidates for 18 days of livetime. Other limits are from AMANDA [14], RICE [15], ANITA-lite [16], Auger [17], HiRes [18], FORTE [13]. The BZ (GZK) neutrino model range is determined by a variety of models [19], [20], [21], [22], [23], [24], [25].

neutrino models. The case of a model which saturates the canonical Waxman-Bahcall flux bounds for both evolved and standard UHECR sources [26] is also included. ANITA-1 imposes strong limits on the highest BZ neutrino models, which require extremely high-energy cutoffs in the parent cosmic-ray source spectral energy distribution. The current limits disfavor UHECR source spectra extending to  $10^{23}$  eV. ANITA-1 sensitivity approaches a class of models here denoted as “strong-source evolution” models, which assume that the UHECR source evolution follows the cosmic evolution of more energetic sources, for example gamma-ray burst host galaxies [27]; these mid-range models are constrained at about the 60% CL but none are ruled out yet. The ANITA-1 90% CL integral flux limit on a pure  $E^{-2}$  spectrum for the energy range  $10^{18.5}$  eV  $\leq E_\nu \leq 10^{23.5}$  eV is  $E_\nu^2 F \leq 2 \times 10^{-7}$  GeV cm<sup>-2</sup> s<sup>-1</sup> sr<sup>-1</sup>.

### III. ANALYSIS DEVELOPMENTS

Two additional analyses, independent from the one discussed above, of the ANITA-1 data are currently underway. The follow up analyses aim to check the results of the first but are also expected to have improved sensitivity. The majority of neutrinos expected to trigger ANITA have signal strengths that are close to thermal noise levels.

Weak radio signals are susceptible to side-lobe reconstructions which discard events that otherwise still contain directional information. To rescue this class of events, an analysis method that relies on radio coherence techniques and associated statistical behavior has been

TABLE II  
EXPECTED NUMBERS OF EVENTS  $N_\nu$  FROM SEVERAL UHE NEUTRINO MODELS, AND CONFIDENCE LEVEL  
 $CL = 100(1 - \exp(-N_\nu))$  FOR EXCLUSION BY ANITA-1 OBSERVATIONS.

Model & references	predicted $N_\nu$	CL,%
<i>Baseline BZ models</i>		
Protheroe & Johnson 1996 [19]	0.22	19.7
Engel, Seckel, Stanev 2001 [20]	0.12	11.3
Barger, Huber, & Marfatia 2006 [25]	0.38	31.6
<i>Strong source evolution BZ models</i>		
Engel, Seckel, Stanev 2001 [20]	0.39	32.3
Kalashiev <i>et al.</i> 2002 [21]	1.03	64.3
Aramo <i>et al.</i> 2005 [23]	1.04	64.6
Barger, Huber, & Marfatia 2006 [25]	0.89	58.9
Yuksel & Kistler 2007 [27]	0.56	42.9
<i>BZ Models that saturate all bounds:</i>		
Kalashiev <i>et al.</i> 2002 [21]	10.1	> 99.99
Aramo <i>et al.</i> 2005 [23]	8.50	> 99.98
<i>Waxman-Bahcall fluxes:</i>		
Waxman, Bahcall 1999, evolved sources [26]	0.76	53.2
Waxman, Bahcall 1999, standard [26]	0.27	23.7

developed. The signal reconstruction relies on measuring the degree of first order coherence in a set of adjacent antennas as a function of the radiation incident angle (see figure 3). The incident angle information is then used to phase together the antenna waveforms resulting in a coherently summed signal (see figure 4). These techniques are expected to reduce the analysis threshold thus improving sensitivity.

An analysis that aims to improve efficiency also runs the risk of accepting more background. For this reason, a statistical approach for thermal noise background rejection is required. The advantage of having reliable statistical measures is that analysis cuts can be tuned to different purposes. For example, a set of cuts can be tuned to establish a limit, detect a neutrino signal, or better understand the distribution of anthropogenic sources on the continent. This approach is important for the analysis of very large data sets where low probability fluctuations that mimic a rare signal can be present. The methods described above are also being applied to the developing ANITA-2 analysis where, given the improvements in instrument sensitivity, such an approach is more relevant.

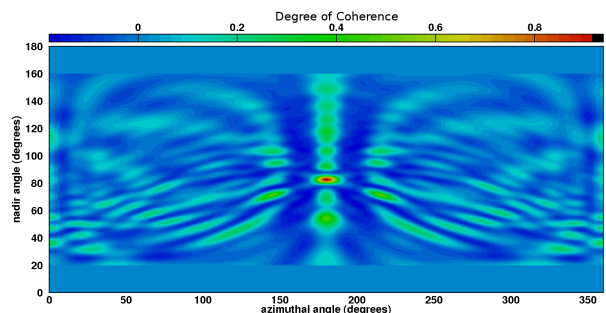


Fig. 3. The averaged coherence of six antenna waveforms showing a peak in the direction of incidence.

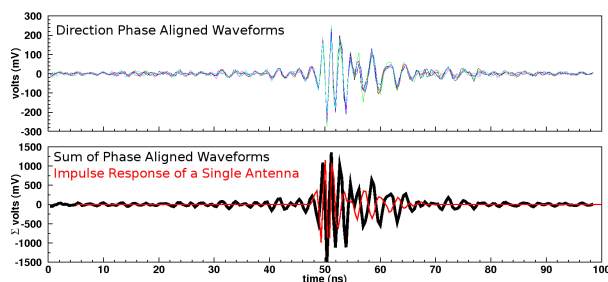


Fig. 4. Top: The six waveforms used in reconstruction phased according to the reconstructed direction. Bottom: The sum of the six waveforms above compared to the instrument's impulse response waveform.

#### IV. THE SECOND ANITA FLIGHT

ANITA-2 was launched from the Long Duration Balloon facility in Williams Field, Antarctica on December 2008 and had a successful 30 day flight over Antarctica and recorded  $\sim 27$ M events. Several hardware improvements including the addition of 8 horn antennas on the bottom of the payload have increased the payload's sensitivity. Unlike the first flight, the second flight had more standard stratospheric conditions leading to a much improved flight path with mostly high quality radio quiet data (see figures 5 and 6) over the deep ice of East Antarctica. Taking all these factors into account, it is expected that ANITA-2 is about a factor of 3 to 8 improvement over ANITA-1.

#### V. SUMMARY

In summary, we have set the strongest bounds to date on the ultra-high energy neutrino flux at energies above  $3 \times 10^{18}$  eV, using the radio Cherenkov method via synoptic observations of the Antarctic ice sheets from stratospheric altitudes. Our methodology appears to have no observed physics backgrounds, but may have detected events due to cosmic-ray extensive air showers that are easily separated from the neutrino events we seek. Additional results from refined independent analyses will be completed soon. The results from the improved ANITA-2 payload and flight path are eagerly awaited.

This work has been supported by the National Aeronautics and Space Administration, the National Science Foundation Office of Polar Programs, the Department of Energy Office of Science High Energy Physics Division, and the UK Science and Technology Facilities Council. Special thanks to the staff of the Columbia Scientific Balloon Facility.

#### REFERENCES

[1] K. Greisen, Phys. Rev. Lett. 16, 748, (1966).  
 [2] G. T. Zatsepin, V. A. Kuzmin, JETP Lett. 4, 78 (1966)[Pisma Zh. Eksp. Teor. Fiz. 4, 114, (1966)].  
 [3] V. S. Beresinsky, G. T. Zatsepin, Phys. Lett. B 28, 423(1969).  
 [4] Phys. Rev. Lett. 101, 061101 (2008)  
 [5] W.M. Yao et al., Journal of Physics G, 33 (2006).  
 [6] D. Seckel, T. Stanev, Phys. Rev. Lett. 95, 141101, (2005).

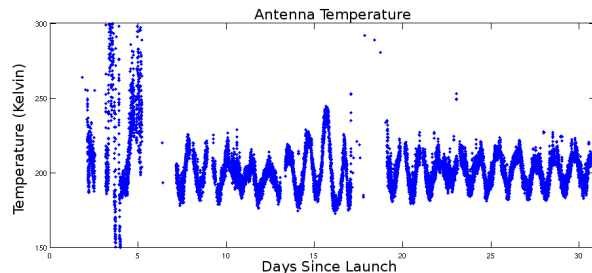


Fig. 5. Plot of the antenna noise temperature for the ANITA-2 flight.

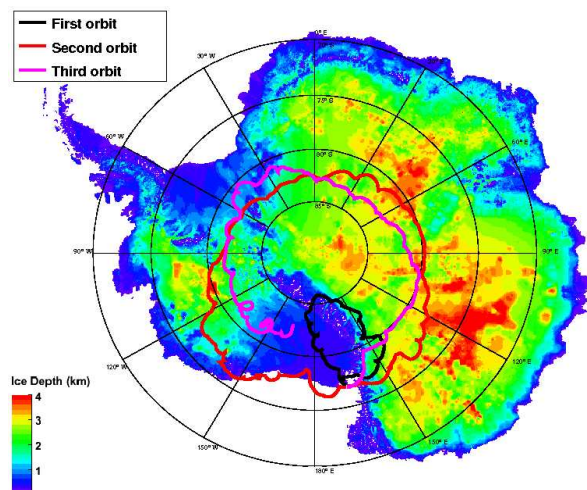


Fig. 6. ANITA-2 flight path and ice depth.

[7] ANITA Collaboration: P. W. Gorham, et al., Phys. Rev. Lett. 99, 171101, (2007).  
 [8] G. A. Askaryan, JETP 14, 441, (1962); JETP 21, 658, (1965).  
 [9] ANITA Collaboration: P. W. Gorham, et al., Phys. Rev. D, submitted 2008; arxiv:0812.1920.  
 [10] J. Nam et al. (ANITA Collaboration), Proceedings of ICRC 2009 (2009)  
 [11] R. Gandhi, Nucl. Phys. Proc. Suppl. 91, (2000) 453, (2000).  
 [12] L. A. Anchordoqui, J. L. Feng, H. Goldberg, A. D. Shapere, Phys. Rev. D 66, 103002,  
 [13] N. Lehtinen, P. Gorham, A. Jacobson, R. Roussel-Dupre, Phys. Rev. D 69, 013008, (2004); astro-ph/030965.  
 [14] IceCube Collaboration: M. Ackermann, et al. Astroph. Journ. 675:1014, (2008).  
 [15] I. Kravchenko, et al., Phys.Rev. D 73, 082002, (2006).  
 [16] ANITA Collaboration: S. W. Barwick et al., Phys. Rev. Lett. 96 171101, (2006).  
 [17] Pierre Auger Collaboration, Phys. Rev. Lett. 100, 211101, (2008).  
 [18] HiRes Collaboration: R. U. Abbassi et al., Ap. J. submitted, 2008; arXiv:0803.0554.  
 [19] R. J. Protheroe, P. A. Johnson, Astropart. Phys. 4, 253, (1996).  
 [20] R. Engel, D. Seckel, T. Stanev, Phys. Rev. D 64, 093010, (2001).  
 [21] O. E. Kalashev, V. A. Kuzmin, D. V. Semikoz, G. Sigl, Phys. Rev. D 66, 063004 (2002).  
 [22] O. E. Kalashev, V. A. Kuzmin, D. V. Semikoz, G. Sigl, Phys. Rev. D 65, 103003, (2002).  
 [23] C. Aramo, et al., Astropart. Phys. 23, 65, (2005).  
 [24] M. Ave, N. Busca, A. V. Olinto, A. A. Watson, T. Yamamoto, Astropart.Phys. 23, 19, (2005).  
 [25] V. Barger, P. Huber, D. Marfatia, Phys.Lett. B 642, 333, (2006).  
 [26] E. Waxman, J. Bahcall, Phys. Rev. D 59, 023002, (1999).  
 [27] H. Yuksel & M. D. Kistler, Phys. Rev. D 75, 083004, (2007) .